CAMS Service Evolution

D3.2 Introduction of EQSAM4Clim inorganic aerosol module into IFS-HAMM7

Due date of deliverable	30 June 2025
Submission date	30 June 2025
File Name	CAMAERA-D3.2-V1.1
Work Package /Task	WP3/T3.2
Organisation Responsible of Deliverable	KNMI
Author name(s)	Swen Metzger, Vincent Huijnen, Ramiro Checa-Garcia, Samuel Rémy
Revision number	V1.1
Status	
Dissemination Level	public

The CAMAERA project (grant agreement No 101134927) is funded by the European Union.
Views and opinions expressed are however those of the author(s) only and do not necessarily reflect those of the European Union or the Commission. Neither the European Union nor the granting authority can be held responsible for them.

Executive Summary

This deliverable fulfils the objectives outlined in the Description of Action (DoA, WP3 T3.2): implementation of EQSAM4Clim into IFS-HAMM7, including potential scaling of prognostic variables and coupling of aerosol precursor gases and bulk aerosol species with the EQSAM4Clim scheme.

Deliverable D3.2 complements the developments of D3.1 by addressing the coupling of secondary inorganic aerosols with precursor gases and mineral cations, as represented in HAMM7, using EQSAM4Clim (Metzger et al., 2018; 2024). This first coupling step has been achieved, and preliminary evaluation results are presented.

EQSAM4Clim-v12 serves as the basis for this work, providing an accurate and computationally efficient method for calculating aerosol composition and acidity. The model employs an analytical approach suitable for both numerical weather prediction and air quality forecasting, free of numerical noise. It resolves gas-liquid-solid and reduced gas-liquid partitioning and associated water uptake, enabling aerosol acidity diagnostics. A comprehensive performance assessment using the EQSAM box model and IFS-COMPO cycle 49R1 is available in Metzger et al. (2023, 2024), Rémy et al. (2024), and Williams et al. (2024).

Key preliminary findings include:

- **HNO_3**: Deviations between a version with EQSAM4Clim activated (E4C) and a reference, without input of chemical speciation of the aerosol input (REF) arise from improved chemical speciation in E4C.
- **NO_3^-**: Differences result from coupling sea salt and dust fluxes in E4C. These extend vertically up to the UTLS, though with reduced magnitude.
- **NH_4^+**: Inverse spatial patterns to NH_3 due to suppression of long-range transport by chemical speciation.
- **SO_2 and SO_4^{2-}**: Largely similar distributions between E4C and REF. Differences over the Northern Hemisphere are likely due to indirect effects via wet chemistry and cloud acidity.
- **O_3**: Differences are overall small for surface and zonal concentrations (< 0.1%).
- **Regional comparison:** The E4C results are closest to EMEP observations over Europe for HNO_3 and $NH_4^+{}_{as}$.

As these are preliminary results, the concentrations shown may evolve with further model refinement, as is planned in the next project phase as part of WP4.

Table of Contents

1 Introduction

1.1 Background

The European Union's flagship Space programme Copernicus provides a key service to the European society, turning investments in space-infrastructure into high-quality information products. The Copernicus Atmosphere Monitoring Service (CAMS, https://atmosphere.copernicus.eu) exploits the information content of Earth-Observation data to monitor the composition of the atmosphere. By combining satellite observations with numerical modelling by means of data assimilation and inversion techniques, CAMS provides in near-real time a wealth of information to answer questions related to air quality, climate change and air pollution and its mitigation, energy, agriculture, etc. CAMS provides both global atmospheric composition products, using the Integrated Forecasting System (IFS) of ECMWF - hereafter denoted the global production system -, and regional European products, provided by an ensemble of eleven regional models - the regional production system.

The CAMS AERosol Advancement (CAMAERA) project will provide strong improvements of the aerosol modelling capabilities of the regional and global systems, on the assimilation of new sources of data, and on a better representation of secondary aerosols and their precursor gases. In this way CAMAERA will enhance the quality of key products of the CAMS service and therefore help CAMS to better respond to user needs such as air pollutant monitoring, along with the fulfilment of sustainable development goals. To achieve this purpose CAMAERA will develop new prototype service elements of CAMS, beyond the current state-of-art. It will do so in very close collaboration with the CAMS service providers, as well as other tier-3 projects. In particular CAMAERA will complement research topics addressed in CAMEO, which focuses on the preparation for novel satellite data, improvements of the data assimilation and inversion capabilities of the CAMS production system, and the provision of uncertainty information of CAMS products.

1.2 Scope of this deliverable

1.2.1 Objectives of this deliverable

The aerosol module in the current global analysis and forecast system in the IFS cycle 49R1, IFS-AER (Rémy et al., 2022; 2024; Metzger et al. 2024), is based on a bin-bulk representation of tropospheric aerosol, with an extension towards stratospheric aerosols. While it is very successful to provide key aerosol air quality information, such as PM2.5 and PM10, along with analyses and forecasts of AOD in the operational context in CAMS, it provides only limited information on the particle size distribution. Moreover, IFS-AER does not account for internal mixing of different chemical components, which has important implications for the way the aerosol optical properties and aerosol-cloud interactions (droplet activation and removal of aerosol by clouds and precipitation) can be described. This impacts the life cycle of the aerosol particles and their direct and indirect radiative effects.

We address these fundamental limitations by the introduction of a modal scheme based on M7 (Tegen et al., 2019) into the IFS, as described in Deliverable report D3.1. However, the default version of HAMM7 does not include a description of the coupling with secondary inorganic aerosol.

This is topic of the current Deliverable. A coupling of secondary inorganic aerosol with precursor gases is established using the EQSAM4Clim scheme (Metzger et al., 2018; 2024). This requires a careful coupling of aerosol precursor gases and mineral cations with individual aerosol types as represented in M7.

1.2.2 Work performed in this deliverable

In this deliverable the work as planned in the Description of Action (DoA, WP3 T3.2) was performed:

Task 3.2: Introduce EQSAM4Clim inorganic aerosol modeling into IFS-HAMM7: Implementation of EQSAM4Clim into IFS-HAMM7, possibly scaling of IFS-HAMM7 prognostic variables to derive some of the anions/cations input of EQSAM4Clim; Coupling of aerosol precursor gases and bulk aerosol species considered in M7 to EQSAM4Clim.

1.2.3 Deviations and counter measures

No deviations have been encountered.

1.2.4 CAMAERA Project Partners

HYGEOS	HYGEOS SARL
ECMWF	EUROPEAN CENTRE FOR MEDIUM-RANGE WEATHER FORECASTS
Met Norway	METEOROLOGISK INSTITUTT
RC-Io	RESEARCHCONCEPTS IO
BSC	BARCELONA SUPERCOMPUTING CENTER-CENTRO NACIONAL DE SUPERCOMPUTACION
KNMI	KONINKLIJK NEDERLANDS METEOROLOGISCH INSTITUUT-KNMI
SMHI	SVERIGES METEOROLOGISKA OCH HYDROLOGISKA INSTITUT
FMI	ILMATIETEEN LAITOS
MF	METEO-FRANCE
TNO	NEDERLANDSE ORGANISATIE VOOR TOEGEPAST NATUURWETENSCHAPPELIJK ONDERZOEK TNO
INERIS	INSTITUT NATIONAL DE L ENVIRONNEMENT INDUSTRIEL ET DES RISQUES - INERIS
IOS-PIB	INSTYTUT OCHRONY SRODOWISKA - PANSTWOWY INSTYTUT BADAWCZY
FZJ	FORSCHUNGSZENTRUM JULICH GMBH
AU	AARHUS UNIVERSITET
ENEA	AGENZIA NAZIONALE PER LE NUOVE TECNOLOGIE, L'ENERGIA E LO SVILUPPO ECONOMICO SOSTENIBILE

2 Description of EQSAM4Clim-v12 (E4C)

Here we provide only a brief description of the most recent version of EQSAM4Clim (v12), which is in the following to be referred to as E4C. For a more complete description of E4C, we refer to the IFS Documentation CY49R1 - Part VIII: Atmospheric Composition.

2.1 Introduction

To address the relevance of gas-aerosol partitioning and aerosol water for climate and air quality studies, the Equilibrium Simplified Aerosol Model (EQSAM) was developed as a compromise between numerical speed and accuracy (Metzger et al., 2002). EQSAM has been widely used in many air quality and climate modelling systems worldwide (Metzger et al., 2018), including the IFS (Flemming et al., 2015) and the OpenIFS (Huijnen et al., 2022). Recently, the EQSAM version for Climate Applications (EQSAM4Clim) (Metzger et al., 2016a) has been implemented in IFS-COMPO. In contrast to EQSAM, EQSAM4Clim is entirely based on a compound specific single-solute coefficient (ν_i), which was introduced in Metzger et al. (2012) to accurately parameterise the single solution hygroscopic growth, considering the Kelvin effect. This ν_i-approach accounts for the water uptake of concentrated nanometre-sized particles up to dilute solutions, i.e. from the compounds relative humidity of deliquescence (RHD) up to supersaturation (Köhler theory).

EQSAM4Clim extends the ν_i-approach to multicomponent mixtures, including semi-volatile ammonium compounds and major crustal elements. The advantage of EQSAM4Clim is that the entire gas–liquid–solid aerosol phase partitioning and water uptake, including major mineral cations, is solved analytically without iterations and thus computationally very efficient. This makes EQSAM4Clim suited not only for climate simulations, but also applicable to high resolution Numerical Weather Predictions (NWP) coupled with comprehensive atmospheric chemistry providing global values of particulate matter, as done in the Copernicus Atmosphere Monitoring Service (CAMS, Peuch et al., 2022; Rémy et al., 2022; Williams et al., 2022; Rémy et al., 2019; Huijnen et al., 2016). The most recent version of EQSAM4Clim (v12) has now been integrated in the operational Cycle 49r1 as part of the recent upgrade to ECMWF's Integrated Forecasting System (IFS), which has been implemented on 12 November 2024.

2.2 General Feature

A schematic of the various input parameters needed for use in E4C is shown in Figure 1, where chemical species from each phase type is given. E4C is based on a compound specific single-solute coefficient (ν_i), which was introduced in Metzger et al. (2012) for single solute solutions and extended to multi-component mixtures by Metzger et al. (2016a) to include semi-volatile ammonium (NH_4^+) compounds and major crustal elements. A feature of the ν_i-approach is that the entire gas–liquid–solid aerosol phase partitioning and water uptake can be solved analytically without iterations, and hence without numerical noise.

E4C takes as input (i) the meteorological parameters air temperature (T) and relative humidity (RH), (ii) the aerosol precursor gases, i.e., major oxidation products of natural sources and anthropogenic air pollution represented by ammonia (NH_3), hydrochloric acid (HCl), nitric acid (HNO_3), sulphuric acid (H_2SO_4), and (iii) the ionic aerosol concentrations, i.e., lumped (both liquid and solid) anions, sulphate (SO_4^{2-}), bi-sulphate (HSO_4^-), nitrate (NO_3^-), chloride (Cl^-), and lumped (liquid+solid) cations, NH_4^+, sodium (Na^+), potassium (K^+), magnesium (Mg^{2+}) and calcium (Ca^{2+}).

The equilibrium aerosol composition and aerosol Associated Water mass (AW) is calculated by E4C through the neutralization of anions by cations, which yields numerous salt compounds, i.e., the sodium salts Na_2SO_4, $NaHSO_4$, $NaNO_3$, NaCl, the potassium salts K_2SO_4, $KHSO_4$, KNO_3, KCl, the ammonium salts $(NH_4)_2SO_4$, NH_4HSO_4, NH_4NO_3, NH_4Cl, the

magnesium salts $MgSO_4$, $Mg(NO_3)_2$, $MgCl_2$, and the calcium salts $CaSO_4$, $Ca(NO_3)_2$, $CaCl_2$. All salt compounds (except $CaSO_4$) can partition between the liquid and solid aerosol phase, depending on T, RH, AW and the temperature-dependent Relative Humidities of Deliquescence of (a) single solute compound solutions (RHD) and (b) of mixed salt solutions.

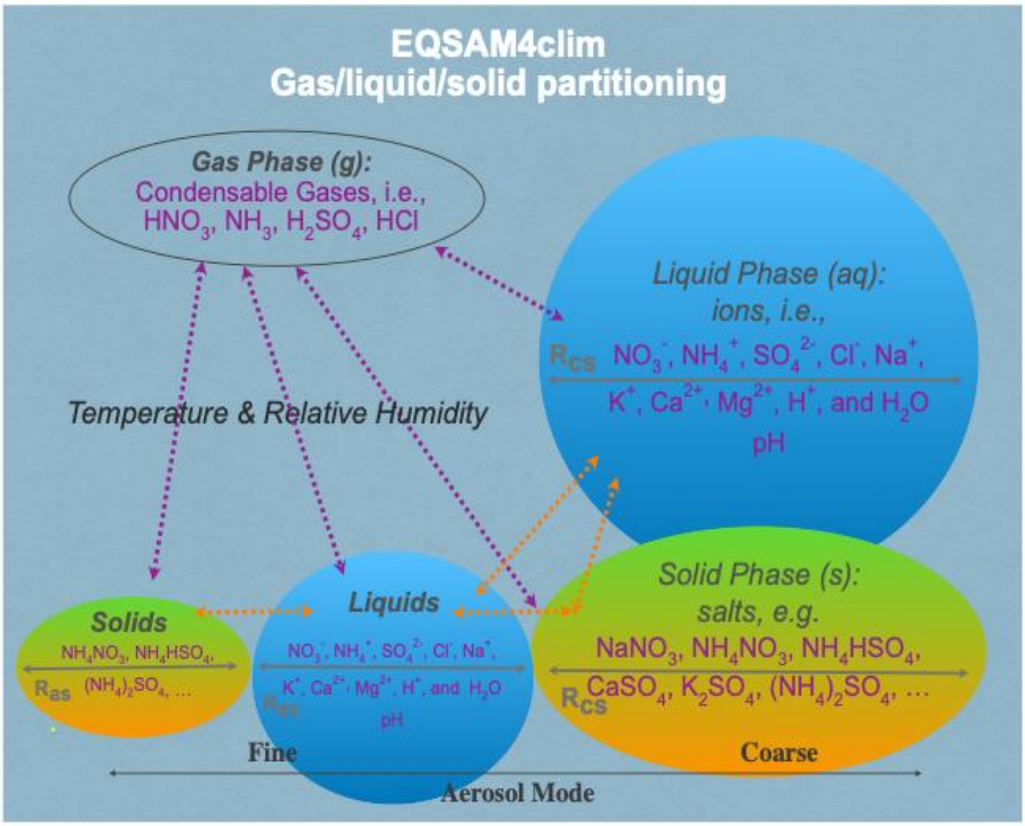

Figure 1: A schematic of the components included in EQSAM4Clim.

Based on the RHD of the single solutes, the (mixed) solution liquid/solid partitioning is calculated, whereby all compounds for which the RH is below the RHD are assumed to be precipitated, such that a solid and liquid phase can coexist. The liquid-solid partitioning is strongly influenced by mineral cations and in turn largely determines the aerosol pH (e.g., Metzger et al., 2006, 2024).

2.3 Recent Updates

E4C estimates the concentration of the hydronium ion (H^+) [mol/m^3(air)] and, subsequently, the pH of the solution from electroneutrality after neutralization of all anions by all cations in the system (following the neutralization reaction order given by Table 3 of Metzger et al. (2016a)). Note that the auto dissociation of H_2O is considered, but currently no dissolution and dissociation of aerosol precursor gases such as sulphur dioxide (SO_2), nitric acid (HNO_3), hydrogen chloride (HCl), or ammonia (NH_3) is taken into account, as this is typically considered in the aqueous phase chemistry module of any global chemistry forecast model.

Originally, the H^+ concentration was obtained directly, from cation-anion neutralization. However, since the neutralization equation does not correct for non-ideal solutions, such as described in Pye et al. (2020) and the references therein, we have introduced with v12 an optional dependency on the aerosol composition, to correct the H^+ concentration (Metzger et al., 2023c). This additional feature is currently not included in cycle 49R1 of IFS-COMPO.

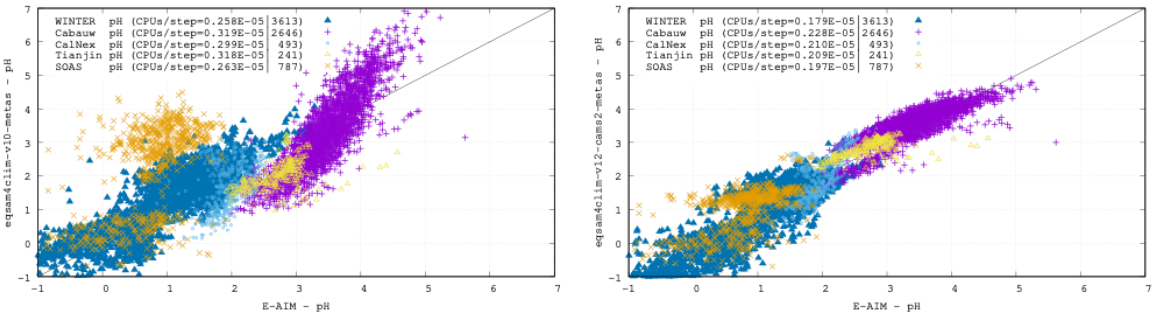

(a) (b)

Figure 2: Comparison of the E4C pH results of v10 (panel a) and v12 (panel b) versus the pH results of the E-AIM reference calculations for all five cases (Metzger et al., 2024). The CPU consumption per step is included for each case. Chip: Apple M1 Ultra; Memory: 128 GB; llvm-11/flang compiler with O3.

Metzger et al. (2024) show an extensive validation against reference model calculations using E-AIM as described in Wexler and Clegg (2002) and Friese and Ebel (2010), using the detailed case study on aerosol acidity provided by Pye et al. (2020). To scrutinize the sensitivity and computational costs of the recent update, the results of two E4C versions including the CPU consumption per step are given in the panels of Figure 2 for the five application cases which are detailed in Pye et al. (2020). Comparing the two E4C versions (left and right panel) shows (a) that the pH results differ mostly for the Cabauw, Tianjin and SOAS campaigns, which represent different aerosol compositions and neutralization levels as defined by where the measurement campaign took place. The Cabauw and Tianjin campaigns represent the most complex aerosol system with SO_4^{2-} being fully neutralized, since both locations are affected by anthropogenic precursors which undergo gas/aerosol partitioning. Conversely, data from the SOAS, CalNex and the WINTER campaigns represent cases where SO_4^{2-} is not fully neutralized. Especially, the measurements from CalNex and the flight during the WINTER campaign represent highly acidic cases.

Additionally, comparing cases shows that (b) the variability in the observed pH ranges across campaigns exceeds the variability in pH simulated by the different modeling code versions. For instance, the pH values are for the WINTER campaign generally much lower compared to e.g., the Cabauw campaign, which shows throughout all results the highest pH values, reflecting the predominance of cations in the aerosol system for the Cabauw case.

Table 1. Statistical metrics for the pH results of E4C pH results of v12 (left) and E-AIM (right column).

Campaign	Data Min		Data Max		Data Mean		Std.-Dev.		Bias	Corr.	Count
Cabauw	1.308	2.000	4.906	5.617	3.575	3.448	0.493	0.521	0.127	0.829	2646
Tianjin	2.171	1.921	3.270	4.565	2.838	2.743	0.250	0.389	0.095	0.595	241
SOAS	-0.719	-0.908	2.622	1.909	0.988	0.763	0.640	0.534	0.225	0.564	787
CalNex	0.428	0.844	3.418	2.836	1.907	1.957	0.649	0.288	-0.05	0.731	493
WINTER	-1.000	-0.996	3.609	3.472	0.934	1.019	0.936	0.831	-0.085	0.874	3613

Table 1 summarizes the key metrics and shows for each campaign the minimum and maximum pH value, together with the data mean and standard deviation for E4C (v12) and E-AIM, as well as the correlation of both. While the data mean is with a variation of less than 0.25 pH units generally satisfactorily close for all campaigns, the correlation coefficient is only above 0.7 for the Cabauw, CalNex and WINTER campaign. Tianjin, which represents besides Cabauw the most complex aerosol system, shows a slightly lower correlation coefficient of 0.6, while SOAS is with a value of 0.56 at the lower end, due to the influence of sulfate/bi-

sulfate partitioning. Bi-sulfates are not always captured in the gas/liquid partitioning compared to cases which include semi-volatile compounds (Cabauw, Tianjin, WINTER). Also note that the correlation coefficient is strongly influenced by the number of data points, such that the WINTER and Cabauw cases are statistically more significant.

The complexity of the Cabauw data is also reflected in the highest computing consumption per step (where CPU/step values are given in the legend within each panel of Figure 2), while the WINTER campaign represents the least complex system (no cations and low temperatures) and, therefore, requires also the least CPU time. Note that there is some uncertainty in these numbers due to the load imbalance of the system ($\leq$ 1%), while the CPU consumption for EQSAM4Clim-v10 is higher because double precision is used. For EQSAM4Clim-v12, the choice of precision is optional and single precision is used throughout this work, since this alone can speed up the computations of up to 50% for these run-time optimized cases.

2.4 Implementation

2.4.1 Coupling of E4C and HAMM7

The microphysical core of HAM is based on M7 (Vignati et al., 2004). It describes sulphate (SO4), black carbon (BC), organic aerosols (OA), sea salt and mineral dust using four water-soluble modes and three water-insoluble modes in different size ranges. In terms of dry particle diameters, the size ranges considered are 0–10 nm (nucleation mode), 10–100 nm (Aitken mode), 0.1–1 μm (accumulation mode) and >1 μm (coarse mode). The nucleation mode only exists for soluble particles. The coupling of E4C with IFS-HAMM7 is done on top of the HAMM7 implementation, which is described in detail in D3.1. The call to the E4C interface is included in the HAMM7 interface, such that E4C can be equally used with either IFS-AER or IFS-HAMM7. The HAMM7 interface has been adopted to accommodate the additional tracer input required for E4C. To enable the gas/aerosol partitioning, the tracers of gases ammonia and nitric acid, and the corresponding aerosol ammonium and nitrate tracers are required and have been added to HAMM7. Currently these are defined in the ‘accumulation soluble’ mode. Also these tracers are subject to dry and wet deposition.
HAMM7, similar as the more comprehensive Global Modal-aerosol eXtension (GMXe) module, calculates the aerosol microphysics, while the underlying gas–liquid–solid aerosol partitioning is calculated by E4C. Compared to HAMM7, GMXe allows a more consistent treatment of major anions and cations and the required chemical speciation (see Section 2.4.2). Still, both aerosol dynamic modules resolve the aerosol size distribution in seven, i.e., four soluble (nucleation, Aitken, accumulation, and coarse) and three insoluble (Aitken, accumulation, and coarse), log-normal modes. Primary particles are emitted in the insoluble modes (Aitken, accumulation, coarse) and only transferred upon chemical aging and transport to the respective soluble modes (Aitken, accumulation, coarse).
The condensation dynamics are calculated within both HAMM7 and GMXe based on a certain number of mono-layers, which determines the coating and thus chemical aging. But only GMXe uses besides sulfuric acid, also nitric acid, hydrochloric acid, ammonia and water vapor as condensable gases, such that coagulation and hygroscopic growth can more effectively alter the aerosol size distributions. Because of the aerosol dynamics, small particles are efficiently transferred to larger sizes, whereby hygroscopic growth of individual aerosol compounds needs to be calculated from aerosol thermodynamics, which is based on a chemical speciation of the aerosol emission fluxes. GMXe has been successfully used to evaluate the Metop PMAp Version 2 AOD Products using Model Data (Metzger et al., 2016b) and to scrutinize the importance of aerosol water for the aerosol optical depth (AOD) calculations using a long-term evaluation of EQSAM4Clim (Metzger et al., 2018).

2.4.2 Chemical aging and speciation of aerosol emissions

The chemical aging process has been activated for the E4C coupling with HAMM7. It is based on explicit neutralization reactions of ions (cations, or anions), which are assigned to the emission fluxes (e.g., K^+, Ca^{2+}, see Metzger et al., 2018). Through the reactions of these cations (anions) with aerosol precursor gases, i.e., major oxidation products of natural and anthropogenic air pollution (i.e., H_2SO_4, HNO_3, HCl, NH_3, and H_2O), various neutralization (salt) compounds can be formed. For E4C, this neutralization process yields numerous salt compounds, i.e., the sodium salts Na_2SO_4, $NaHSO_4$, $NaNO_3$, NaCl, the potassium salts K_2SO_4, $KHSO_4$, KNO_3, KCl, the ammonium salts $(NH_4)_2SO_4$, NH_4HSO_4, NH_4NO_3, NH_4Cl, the magnesium salts $MgSO_4$, $Mg(NO_3)_2$, $MgCl_2$, and the calcium salts $CaSO_4$, $Ca(NO_3)_2$, $CaCl_2$. All salt compounds (except $CaSO_4$) can partition between the liquid and solid aerosol phase, depending on temperature (T), relative humidity (RH), AW and the temperature-dependent Relative Humidities of Deliquescence of (a) single solute compound solutions (RHD) and (b) of mixed salt solutions (MRHD).

From all possible compounds, most relevant for the chemical aging of atmospheric dust particles are calcium sulfate ($CaSO_4$), calcium nitrate ($Ca(NO_3)_2$), calcium chloride ($CaCl_2$). The latter two salts can cause an uptake of water vapor (H_2O) at different ambient humidity, with $CaCl_2$ at RHs as low as 28%. All salt solutions are subject to the RH and T–dependent gas-liquid-solid partitioning that is based on state-of-the-art aerosol thermodynamics.

HAMM7 only treats bulk aerosols (sulfate, sea salt, black and organic carbon, mineral dust) and does not resolve all chemical details as, for instance, GMXe (Pringle et al., 2010a,b; Metzger and Lelieveld, 2007). GMXe consistently considers throughout all aerosol dynamical processes (condensation, inter and intra-modal coagulation, hygroscopic growth) all inorganic and organic anions and cations that are considered in EQuilibrium Simplified Aerosol Model version 3 (EQSAM3). This difference with respect to HAMM7 has important implications for the regional and temporal variability of the aerosol size-distribution, which is largely determined by the chemical aging of aerosols. This aging process depends on the amounts of available condensable compounds that are the outcome of various emission processes and chemistry calculations of IFS.

2.5 Technical integration of E4C

Our initial implementation of HAMM7 was prepared in cycle CY49R1.1 of the IFS. As described in D3.1, we start off from branch nk9_CY49R1.1_GHG_rean_v0. In cycle 49R1, the representation of aerosol, cloud and rain acidity has been improved in IFS-COMPO through the implementation of E4C.

A schematic of the integration of EQSAM4Clim (E4C) into IFS-COMPO is shown in Figure 3. E4C takes the following as input for each model time step and within a given grid box:

(i) *T* and RH as provided by the meteorological component of IFS-COMPO;
(ii) the aerosol precursor gases, i.e., major oxidation products of natural and anthropogenic air pollution represented by NH_3 and HNO_3 (and in future also HCl) from the tropospheric chemistry module IFS(CB05); and
(iii) the ionic aerosol concentration lumped (liquid+solid) anions sulfate (SO_4^{2-}), nitrate (NO_3^-), and chloride (Cl^-), as well as the lumped (liquid+solid) cations ammonium (NH_4^+), sodium (Na^+), potassium (K^+), magnesium (Mg^{2+}), and calcium (Ca^{2+}) as provided by IFS(HAMM7).

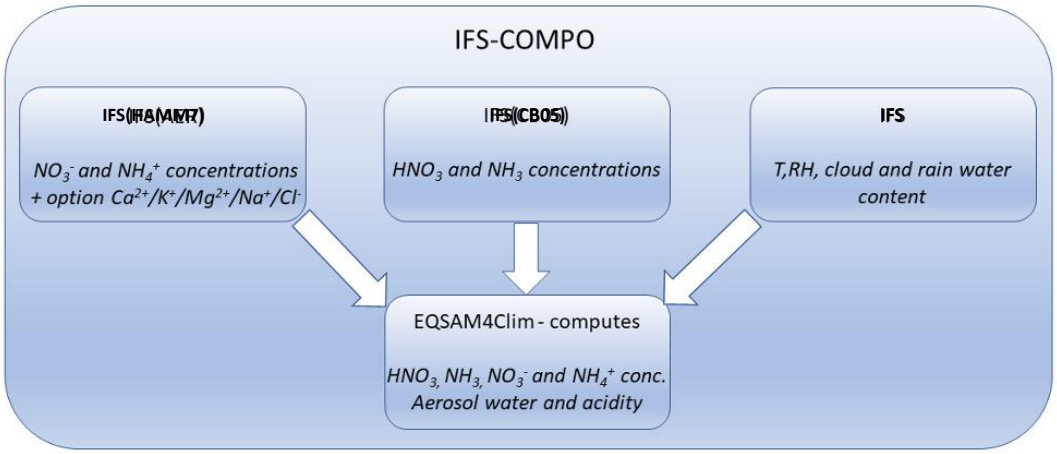

Figure 3. Schematic showing the inputs and outputs of EQSAM4Clim (E4C) as implemented into IFS-COMPO. Figure from Rémy et al., (2024) adopted for current usage of E4C with HAMM7 (default IFS option is AER/E4C).

To activate E4C as part of HAMM7, we have adopted the HAMM7 interface, hamm7_interface.F90, to accommodate the call to the E4C interface, aer_EQSAM4Clim_ifs.F90. The actual gas/aerosol partitioning calculations are done with the E4C module, aer_EQSAM4Clim.F90 (see Table 2).
These have been initially implemented in branch nk9_CY49R1.1_m7dev_v1c_E4Cprep.

Table 2. Overview of the IFS E4C routines used for coupling with HAMM7.

IFS	Purpose and comments
m7/hamm7_interface.F90	Aerosol conversion in atmosphere, and diagnostics. Routines called through aer_phy3_layer.F90
aer_EQSAM4Clim_ifs.F90	E4C interface used for either HAMM7 or AER
aer_EQSAM4Clim.F90	E4C routine used for either HAMM7 or AER

To accommodate the chemical speciation as used in Metzger et al. (2018), we also use scaling factors, which have been derived for the IFS application from recent literature describing EC-Earth (Myriokefalitakis et al., 2022). Here we derive the cation input for EQSAM4Clim, i.e., Ca^{2+}, Mg^{2+} and Na^+ of sea-salt aerosols, and the cation K^+ as a proxy for organic matter (OM) and black carbon (BC) neutralisation potential.

The extra input to EQSAM4Clim are (Rémy et al., 2024):

- Cl^-, taken as 12.8% of sea-salt aerosol,
- Na^+, taken as 7% of sea-salt aerosol and 1.2% of desert dust,
- K^+, taken as 1.5% of desert dust and 3% of organic matter and black carbon,
- Ca^{2+}, for which the calcite fraction of dust input is used, as described in 2.1.1,
- Mg^{2+}, taken as 1.1% of desert dust, following Shah et al. (2020).

Because some IFS-COMPO aerosol species, such as black carbon, organic matter and secondary organics are only used in HAMM7, but not within EQSAM4Clim, an amount of diagnostic aerosol water could still be computed using RH dependent growth factors. They contribute to the estimation of aerosol acidity; see Metzger et al. (2023, 2024) for details on how aerosol / cloud / precipitation pH is computed in IFS-COMPO.

In CY49R1, a measure of hydrophilic growth for dust could be used in the desert dust optical properties, as well as in dry deposition. However, this is not part of this deliverable but might be addressed in a later stage.

3 Evaluation

3.1 Experiment Setup

For the evaluation of the technical E4C coupling with HAMM7, we have setup three model experiments for the period December 2018, which will be evaluated in terms of global gas/aerosol distributions.

The model experiments have been setup as series of 24h forecasts initialized by ERA5 meteorology. The model uses T255 horizontal resolution, with standard 137 levels in the vertical. Table 3 lists the three experiments that are analyzed in this report. The experiments REF and E4C both include the E4C parameterization, but only E4C assesses the impact of using the coupling with online emission fluxes of sea salt and mineral dust and the associated chemical speciation (described above). Please note that both experiments only differ by the coupling of online emission with the E4C interface (which is required for chemical speciation), and the calculation of the tracer tendencies for nitrogen compounds (ammonia, ammonium, nitric acid and aerosol nitrate). All other HAMM7 related processed are the same. For reference also the experiment without E4C (NO_E4C), is also included. For the latter, there is no ammonium and nitrate aerosol in HAMM7.

Table 3: Overview of experiments evaluated in this report.

Exp id / name	Specifics
NO_E4C | b2rn	HAMM7, without any E4C coupling
REF | iqi9	HAMM7 with E4C, but no chemical speciation
E4C | b2ro	HAMM7 with E4C, with chemical speciation

3.2 Global Analysis

3.2.1 Mass diagnostics

We start with a short analysis of the mass diagnostics from the three experiments, Tables 4 and 5. For this we use the last 11 days in December 2018, i.e. after a 20-day spin-up period. We realize that this spin-up is short, and also the 11-day period that is assessed is very short to make quantitative statements on annual total budgets. The 11-day totals are converted into annual total numbers by scaling with a factor [365/11]. The lifetimes in the tables are computed by dividing the loss due to dry and wet deposition and sedimentation by the tropospheric burden. Despite these limitations, this analysis is sufficient for the purpose here, which is to verify the implementation, and assess the differences between the experiments.

Experiment E4C has about 5x larger production of $NO_3^-\_as$ as a consequence of the activation of the chemical speciation, Table 4. With the increase of the production, also the various loss terms due to dry and wet deposition, and sedimentation, is increased. The lifetime of $NO_3^-\_as$ is estimated about 5 days, which appears reasonable. In contrast to nitrate, the $NH_4^+\_as$ production is about 40% lower in E4C compared to REF, Table 5.

Table 4. Production and loss budgets for NO_3^-_as in the various experiments. Units are in [Tg N/yr] unless indicated differently.

	NO_E4C	REF	E4C
Production	-	3.8	18.9
dry deposition	-	0.2	1.1
wet deposition	-	3.1	16.8
sedimentation	-	0.1	0.2
trop. burden [Tg]	-	0.06	0.25
lifetime [days]	-	6.9	5.0

Table 5. Production and loss budgets for NH_4^+_as in the various experiments. Units are in [Tg N/yr] unless indicated differently.

	NO_E4C	REF	E4C
Production	-	16.4	9.5
Dry deposition	-	1.3	0.6
Wet deposition	-	13.8	7.8
Sedimentation	-	0.2	0.1
Trop. burden [Tg]	-	0.24	0.16
Lifetime [days]	-	5.6	6.7

The figures in the following subsections illustrate the global monthly mean distribution over the surface and zonal mean, for December 2018. Here only the species that are key for the gas/aerosol partioning are shown, i.e., accumulation mode ammonium (NH_4^+_as), accumulation nitrate (NO_3^-_as), and accumulation sulfate (SO_4^{2-}_as), as well as their precursor gases ammonia (NH_3), nitric acid (HNO_3), and sulfur dioxide (SO_2). Additionally, we show the ozone concentration (O_3). For each variable, the results of the E4C experiment is shown on the left column, the results of the REF experiment shown in the middle panel, and their difference, i.e., E4C-REF are shown on right figure columns. For comparison, the results of the experiment without any E4C coupling (NO_E4C) is shown versus REF for the aerosol precursor gases NH_3 and HNO_3. The corresponding aerosol figures are omitted, because of missing results.

For easier comparison, all mass mixing ratios (mmr, in kg/kg) are scaled by a variable factor and shown on fixed contour levels (1 to 100). The actual scaling factors used are shown in each figure caption. Please note that with this evaluation, we focus on the technical evaluation and thus on the differences in the spatial patterns of the relevant aerosols and precursor gases. The comparison of the absolute values with observations will be subject to the final verification deliverable.

3.2.2 Nitric Acid

Figure 4a shows the monthly mean HNO_3 surface mmr of NO_E4C (top row) and E4C (bottom row) compared to the REF simulation. Figure 4b shows the corresponding zonal mean distributions. While for the case NO_E4C vs REF differences are most noticeable for the densely populated regions, the most notable deviations occur for the E4C vs REF case over the coastal regions, both reaching differences of up to -200% and regionally even more. These differences are for the former case merely a result of the gas/aerosol partitioning (through E4C), and for the latter case only due to the chemical speciation that is considered in E4C but not in REF. Figure 4b demonstrates that these changes are not limited to the surface concentrations, but also extent into the vertical up to the UTLS.

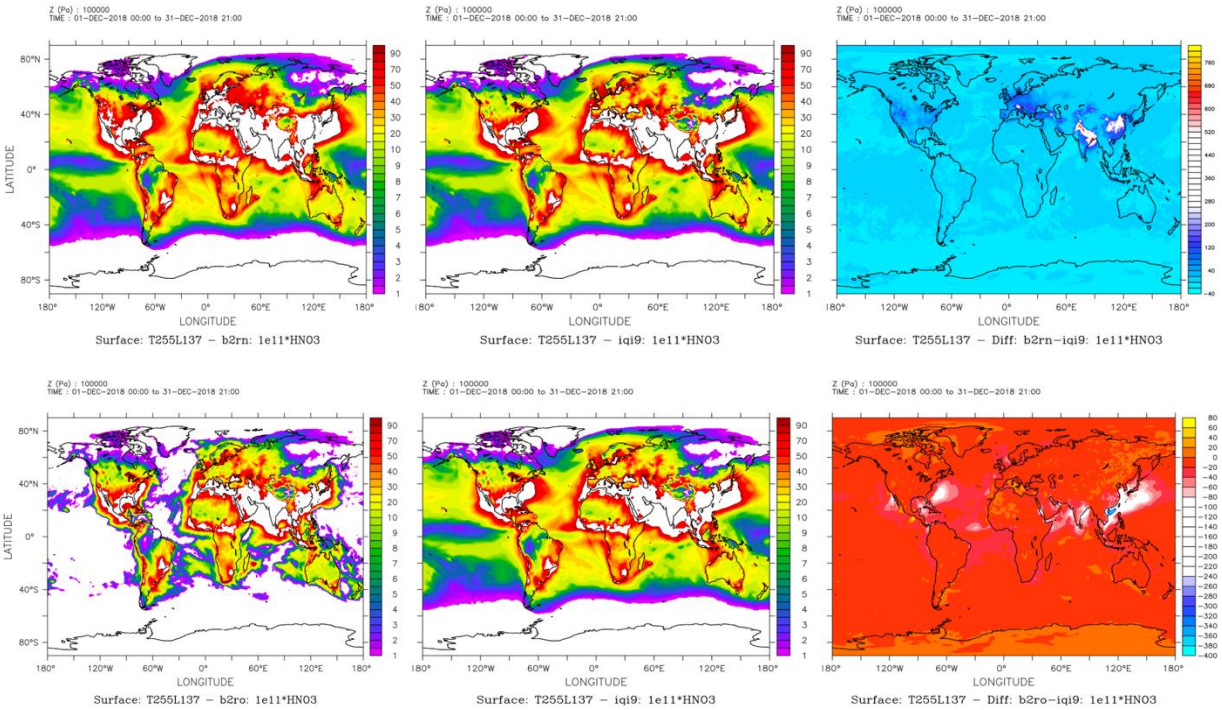

Figure 4a. Surface mean HNO_3 mass mixing ratios. Top row: NO_E4C (left), bottom row: E4C (left); both vs REF, (middle) for Dec 2018 (monthly mean) and the % differences of NO_E4C-REF and E4C-REF (right). mmr are scaled by 1e11 and shown on fixed contour levels (1 to 100).

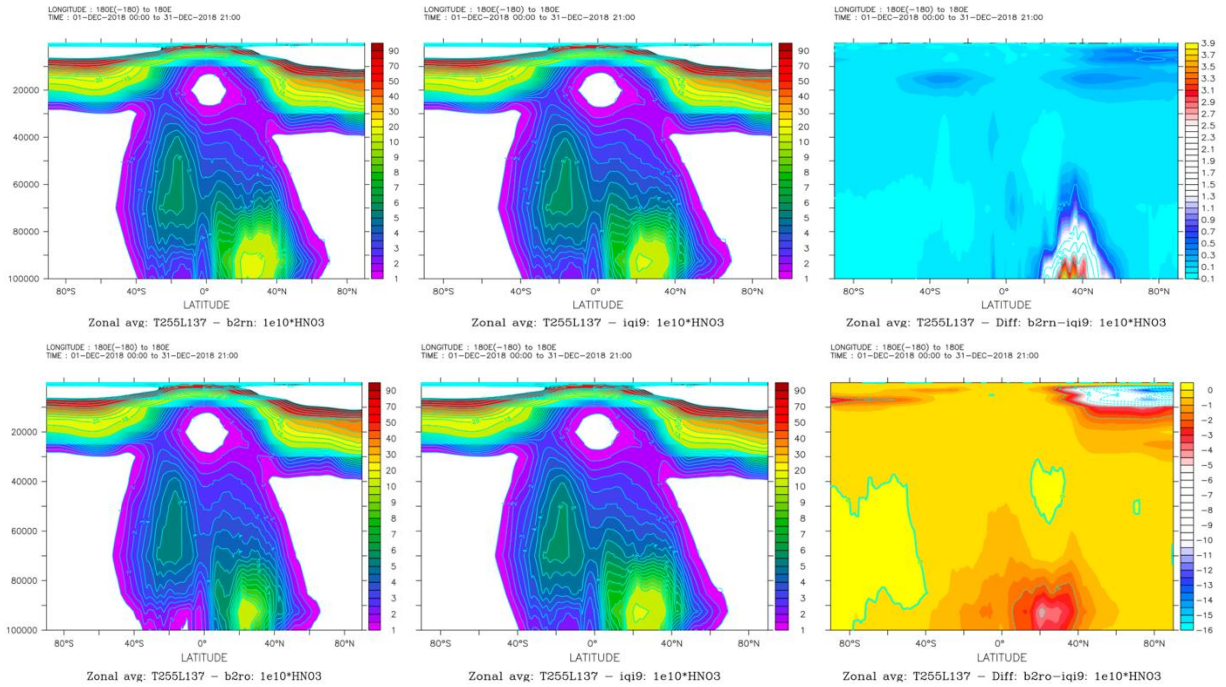

Figure 4b. Zonal mean HNO_3 complementing Figure 4a. Concentrations are scaled by 1e10.

3.2.3 Aerosol nitrate (accumulation mode)

Figure 5a displays the surface accumulation mode concentrations of aerosol nitrate, NO_3^-_as. Figures 5b shows the corresponding zonal mean distributions. Values are markedly higher in E4C than in REF, globally. These differences are merely a result of the chemical speciation that is considered in E4C but not in REF. That is, for REF, there is no coupling of the online sea salt and dust emission fluxes and thus no chemical speciation. Figure 5b demonstrates that these changes are not limited to the surface concentrations, but also extent into the vertical until to the UTLS, although with a much smaller but still significant effect (>100% for the zonal mean and about 10% for the UTLS).

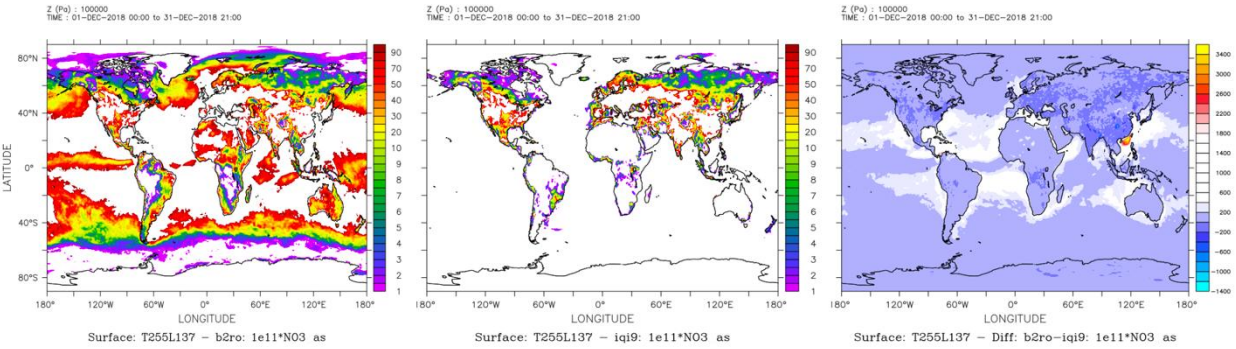

Figure 5a. Surface mean NO_3^-_as of E4C (left) vs REF, (middle) for Dec 2018 (monthly mean) and the % differences of E4C-REF (right). mmr are scaled by 1e11 and shown on fixed contour levels (1 to 100).

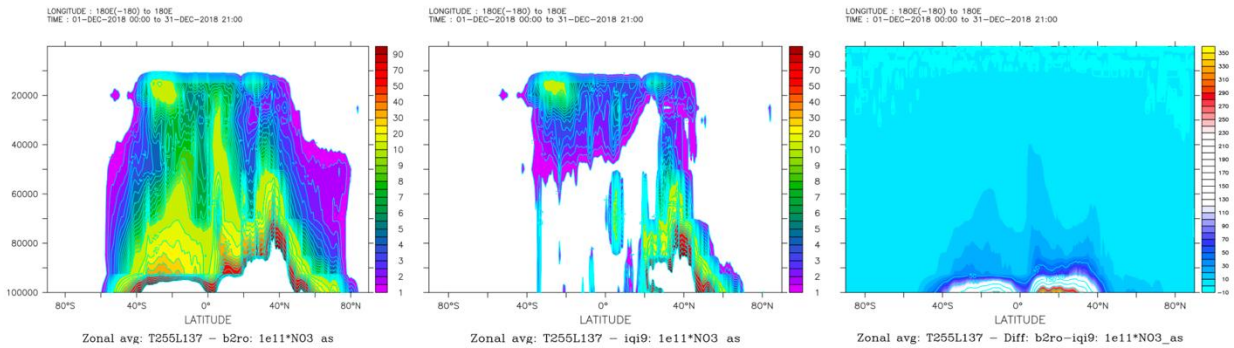

Figure 5b. Zonal mean fine mode NO_3^-_as complementing Figure 5a. mmr are scaled by 1e11.

3.2.4 Ammonia

Figures 6a and 6b depict the surface and zonal mean NH_3 of NO_E4C (top row) and E4C (bottom row) compared to the REF simulation for December 2018. Both experiments regionally differ relative to REF, especially over the oceans. Compared to run NO_E4C, run REF shows lower burden of NH_3 due to activation of ammonium production. Interestingly, E4C partially reverses this pattern, because of the chemical speciation that is the only difference relative to REF.

E4C simulations again show deviations of locally larger than 100%, which also extend into the vertical up to the UTLS for the same reason as described for HNO_3. Because of the different emission sources of NH_3 and HNO_3, both the regional patterns and the magnitude of the differences differ. Most striking here is the enhanced transport of the NH_3 concentrations which extends for the E4C simulation over the oceans. This effect can be explained by the chemical speciation as it largely affects the gas/aerosol partitioning of ammonium nitrate. The additional mineral cations (Na^+, K^+, Mg^{2+}, Ca^{2+}), which are only considered for E4C case, can drive NH_4^+_as out of the aerosol into the gas phase, if either one or all these cations are present (depending on the actual concentrations). But in case of high sea salt aerosol loading, this is likely the case and thus most visible over the windier regions over the oceans. However, due to the fact these are preliminary results, the overall distribution and magnitude of the effect can change. Therefore, these results should not overinterpreted at this stage, but the tendency of the patterns discussed will likely not change.

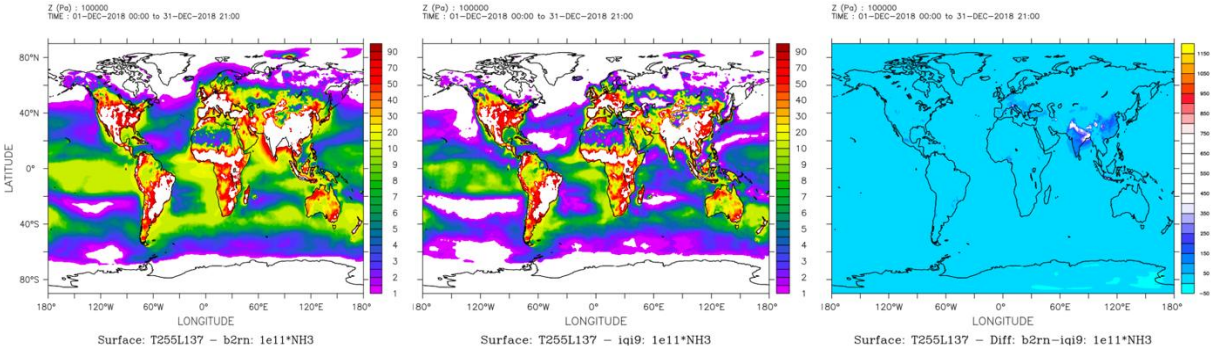

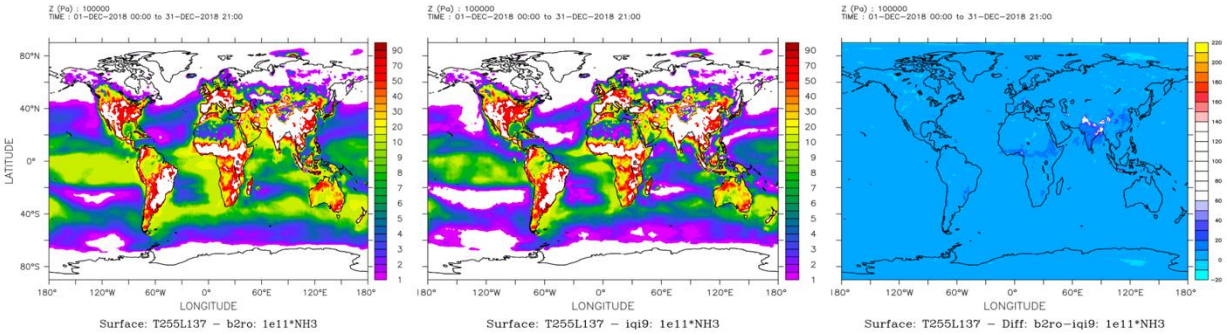

Figure 6a. Surface mean NH_3. Top row: NO_E4C (left), bottom row: E4C (left); both vs REF, (middle) for Dec 2018 (monthly mean) and the differences of NO_E4C-REF and E4C-REF (right). Concentrations are scaled by 1e11 and shown on fixed contour levels (1 to 100).

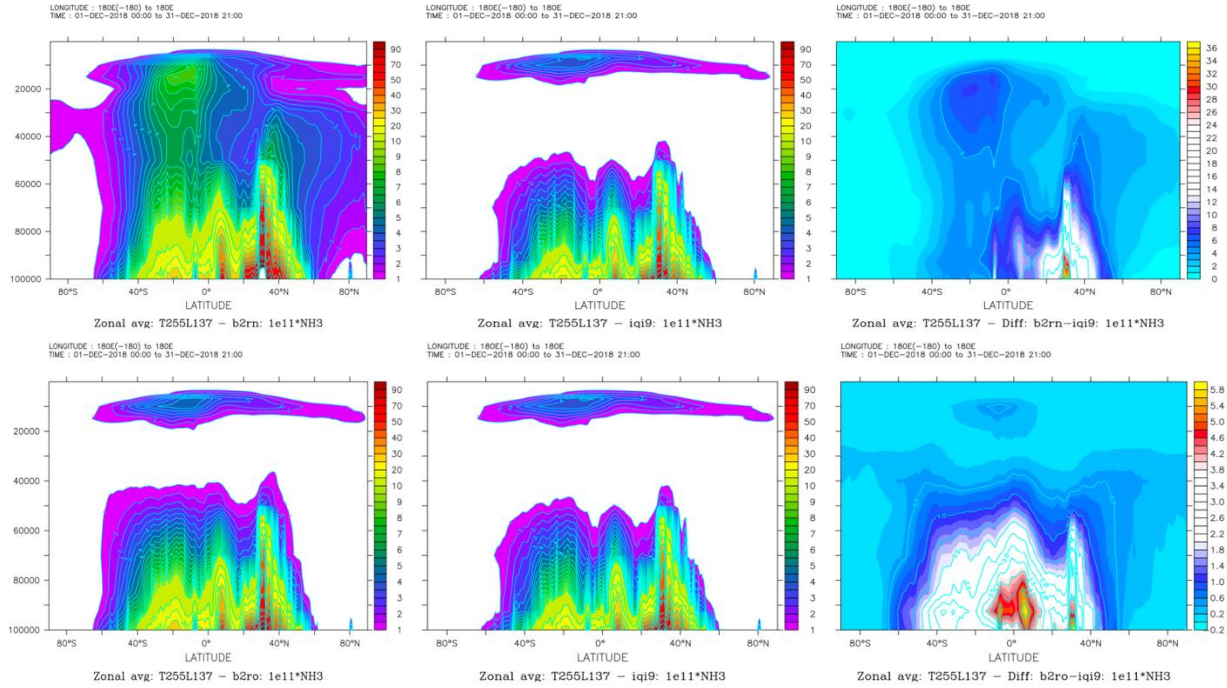

Figure 6b. Zonal mean NH_3 complementing Figure 6a. Concentrations are scaled by 1e11.

3.2.5 Aerosol ammonium (accumulation mode)

Figures 7a and 7b show the corresponding $NH_4^+\_as$ surface and zonal distributions for December 2018 (monthly mean). E4C simulations are consistently inverse to the NH_3 distributions for the same reason as discussed above. Basically, the chemical speciation suppresses the long-range transport of $NH_4^+\_as$, which result into differences up to 100% for the surface, with differences of up to 35% in the zonal mean.

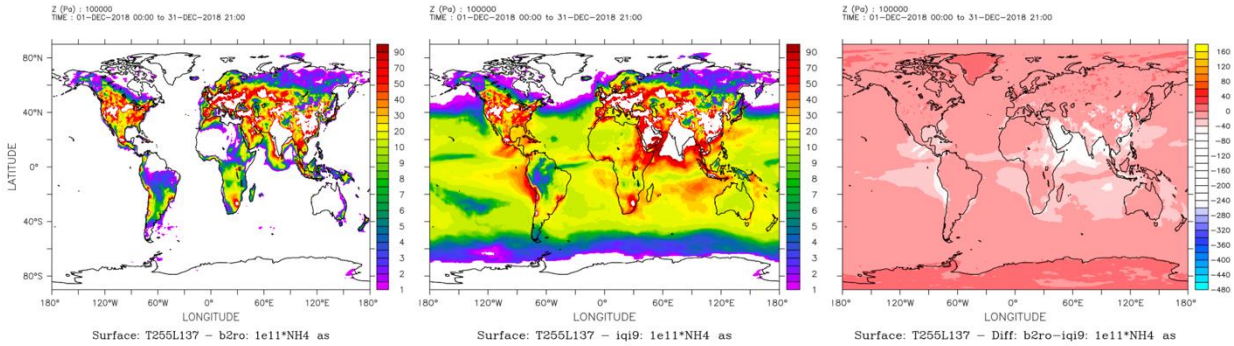

Figure 7a. Surface mean NH_4^+_as of E4C (left) vs REF (middle) for Dec 2018 (monthly mean) and the differences of E4C-REF (right). Concentrations are scaled by 1e11 and shown on fixed contour levels (1 to 100).

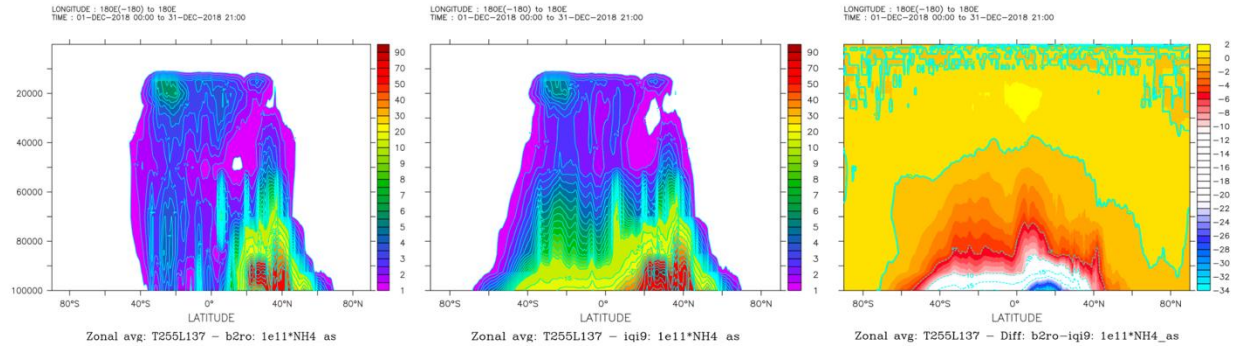

Figure 7b. Zonal mean NH_4^+_as complementing Figure 7a. Concentrations are scaled by 1e11.

3.2.6 Sulfur dioxide

Figures 8a and 8b illustrate the corresponding SO_2 distributions, showing only minor differences for E4C compared to REF, which is consistent with the non-volatile nature of sulfate aerosols and minimal gas/aerosol partitioning influence. The only notable differences (> 10%) are found in East China and for the zonal mean over the Northern Hemisphere (< 2%). These changes are a result of the indirect effect of changes in the acidity, which is calculated within the wet chemistry routine, and which affects the sulfur dioxide oxidation into aerosol sulfate and wet scavenging. And, since the acidity depends on the overall aerosol loading, it is also influenced by the gas/aerosol partitioning of ammonium nitrate aerosols discussed above. But again, the results are preliminary and a full coupling of the aerosol pH from E4C as described in Rémy et al. (2024) and Williams et al. (2024) is not yet considered.

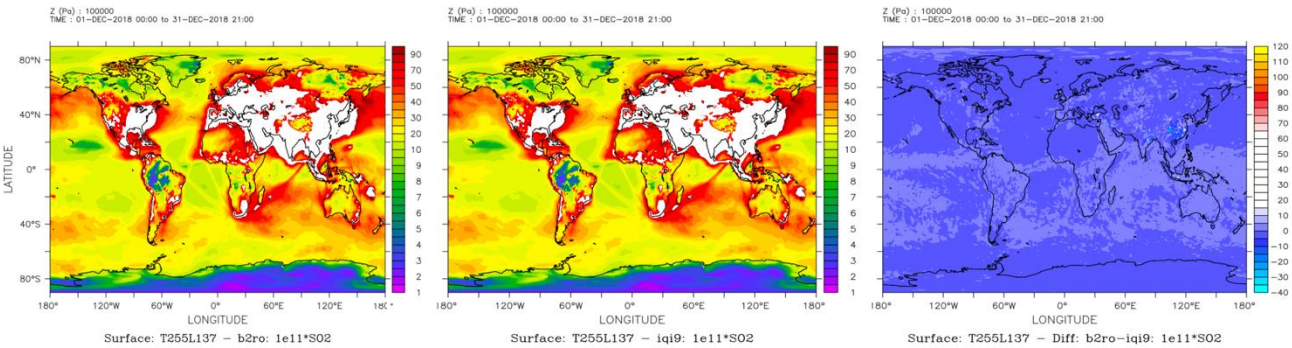

Figure 8a. Surface mean SO_2 of E4C (left) vs REF (middle) for Dec 2018 (monthly mean) and the differences of E4C-REF (right). Concentrations are scaled by 1e11 and shown on fixed contour levels (1 to 100).

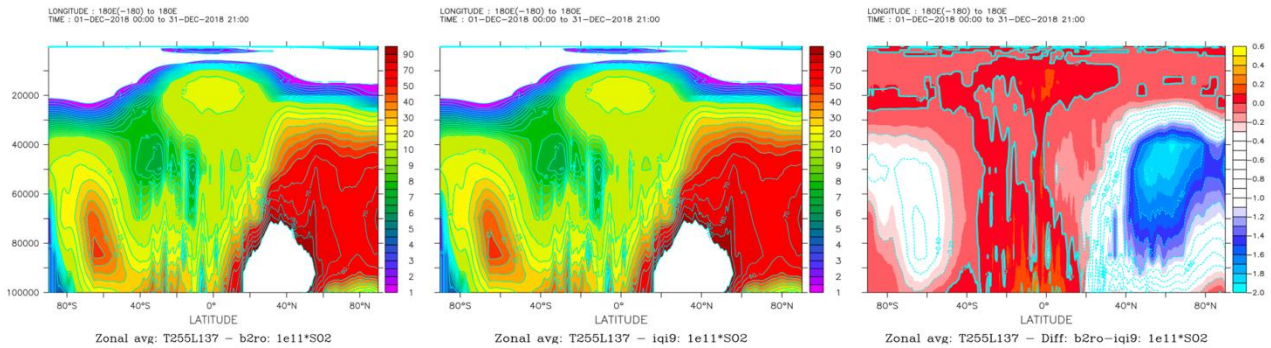

Figure 8b. Zonal mean SO_2 complementing Figure 8a. Concentrations are scaled by 1e11.

3.2.7 Aerosol sulfate (accumulation mode)

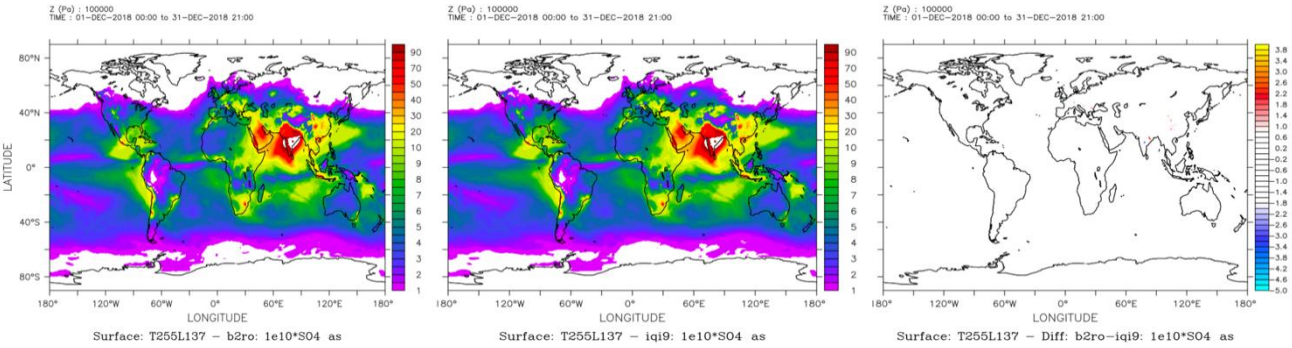

Figure 9a. Surface mean $SO_4^{2-}{}_{as}$ of E4C (left) vs REF (middle) for Dec 2018 (monthly mean) and the differences of E4C-REF (right). Concentrations are scaled by 1e10 and shown on fixed contour levels (1 to 100).

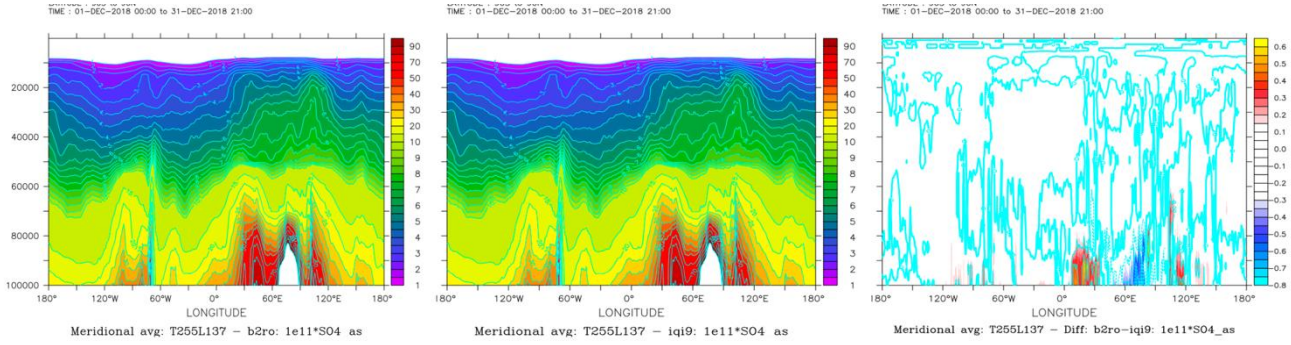

Figure 9b. Zonal mean fine mode $SO_4^{2-}{}_{as}$ complementing Figure 9a. Concentrations are scaled by 1e11.

Figure 9a displays the surface accumulation mode concentrations of aerosol sulfate, $SO_4^{2-}{}_{as}$. Figure 9b shows the corresponding zonal mean distributions. Although the differences are overall negligible for the same reason as discussed above for SO_2, most notable deviations (less than 1%) occur in the zonal mean over the Northern Hemisphere. Because of the non-volatile nature of sulfate aerosols, only a minimal gas/aerosol partitioning influence is expected through the pH-wet chemistry feedback loop that affects the scavenging and oxidation of aerosol precursor gases, including SO_2.

3.2.8 Ozone

Finally, we evaluate the model simulation for a trace gas that is not directly impacted by the gas/aerosol partitioning of nitrogen compounds, i.e., ozone. Figures 10a and 10b show

December 2018 O_3 surface and zonal mean distributions. The E4C and REF simulations are more or less very close for the surface and zonal mean (differences are below 0.1%), but deviations appear along and south of the Intertropical Convergence Zone (ITCZ). This confirms that the current implementation is stable, although future work is needed to fully assess the impact of these changes on ozone chemistry.

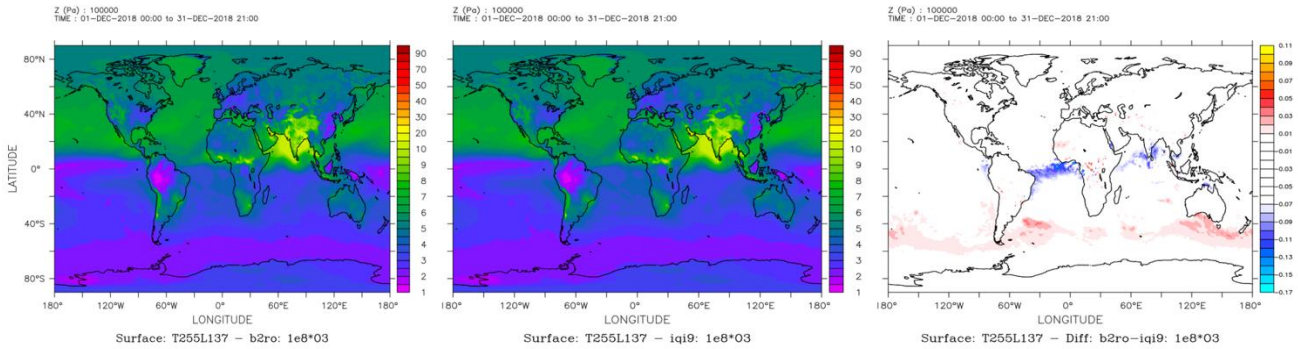

Figure 10a. Surface mean O_3 mmr of E4C (left) vs REF (middle) for Dec 2018 (monthly mean) and the differences of E4C-REF (right). mmr are scaled by 1e8 and shown on fixed contour levels (1 to 100).

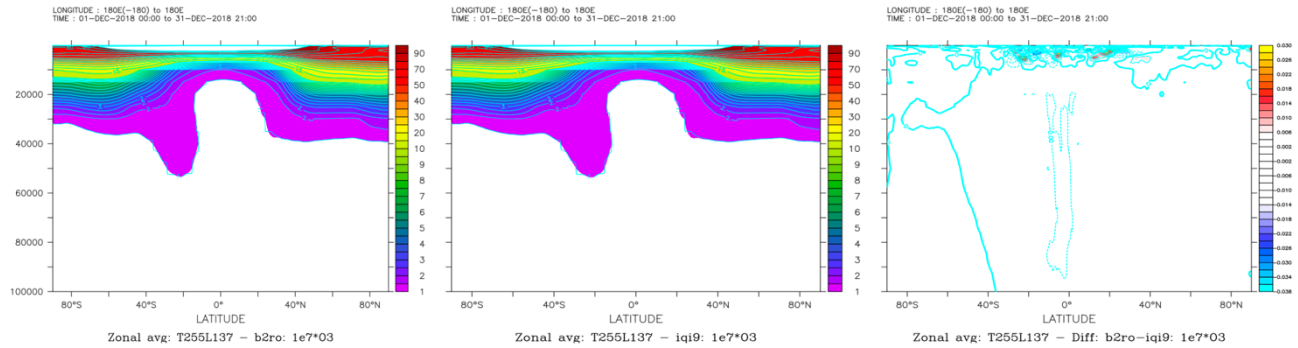

Figure 10b. Zonal mean O_3 complementing Figure 10a. mmr are scaled by 1e7.

3.3 Regional Analysis

Finally, Figure 11 shows the surface concentrations of the semi-volatile species that are key for the gas/aerosol partioning, i.e., accumulation mode ammonium (NH_4^+_as), accumulation nitrate (NO_3^-_as), as well as their precursor gases ammonia (NH_3), nitric acid (HNO_3). The simulation results of NO_E4C (blue), E4C (red) and REF (green) are shown for Europe, December 2018, in comparison to daily measurements of the EMEP measurement network as stored on the EBAS data archive (EMEP https://ebas.nilu.no/). For NH_3(g)/NH_4^+_as and HNO_3(g)/NO_3^-_as couples, the evaluation results are shown as the station average of 49 individual stations located in 10 different countries in Europe. The sampling locations are mostly in Northern and Eastern Europe, but for this preliminary evaluation, the comparison is indicative though valid (despite the short evaluation period).

While for the NO_E4C simulation, the gas phase concentrations are highest, as expected, the corresponding aerosol concentrations are zero (since not activated). The REF and E4C (which includes chemical speciation) experiments show slightly different performance compared to EMEP observations, but generally much improved compared to NO_E4C for NH_3 and HNO_3. These preliminary results indicate that the tracer coupling in terms of chemical speciation can be important to yield realistic gas and aerosol concentrations, also depending on the location. Therefore, this aspect is also subject for further improvements.

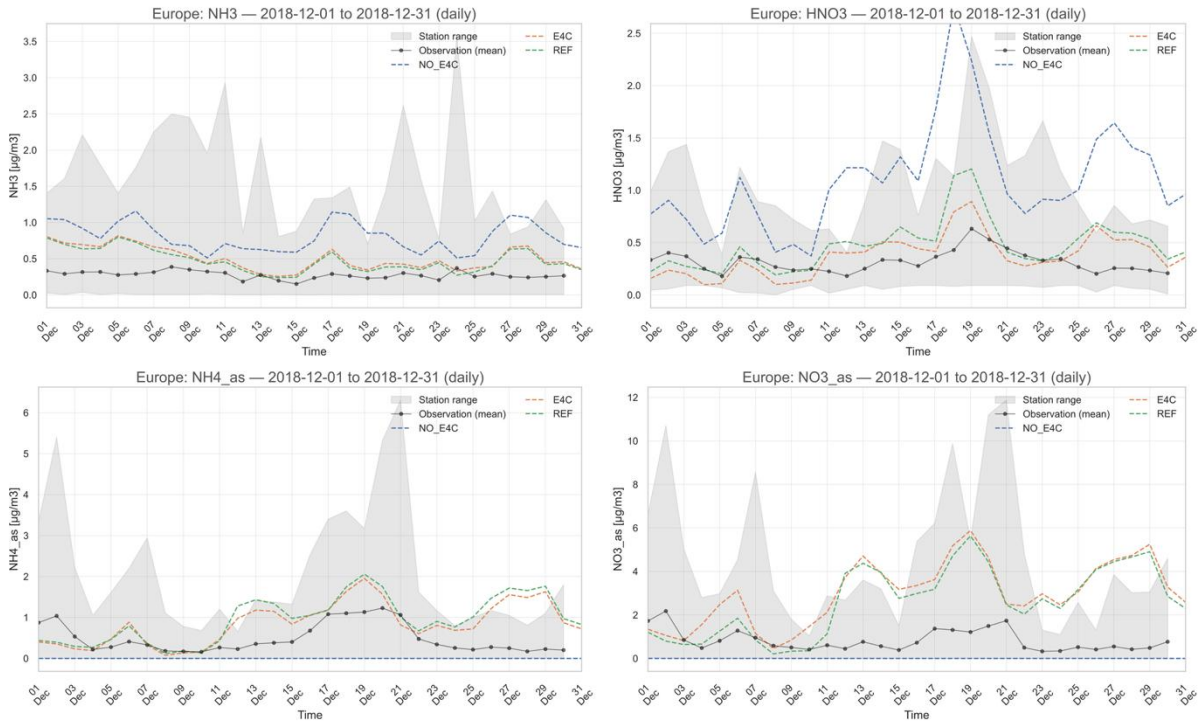

Figure 11. Surface concentrations of NO_E4C, E4C vs REF for Europe and Dec 2018. The semi-volatile aerosols and their precursor gases are shown in comparison to EMEP measurements: NH_3 (upper left) and HNO_3 (upper right), NH_4^+_as (lower left) and NO_3^-_as (lower right). Concentrations are shown in µg/m^3.

4 Conclusion

This deliverable fulfils the objectives defined in the Description of Action (DoA, WP3 T3.2): implementation of EQSAM4Clim (E4C) into the IFS-HAMM7 aerosol module, including coupling of aerosol precursor gases and bulk aerosol species, and derivation of anion/cation inputs.

A first implementation of E4C into the HAMM7 module (CY49R1 of IFS) was achieved. The gas/aerosol partitioning of ammonia and nitric acid shows reasonable global distributions, although absolute concentrations remain preliminary.

Key findings include:

- **HNO_3** : Surface deviations up to -200% over coastal regions due to the gas/aerosol partitioning calculation (through E4C) and E4C's detailed chemical speciation, with smaller impacts (~-5% zonal mean; <2% in the UTLS).
- **NO_3^-_as**: Differences stem from missing speciation in REF, especially the uncoupled sea salt and dust fluxes. Zonal mean changes exceed 100%;
- **NH_3**: Surface deviations >100%, with enhanced vertical transport over oceans in E4C due to ammonium nitrate partitioning affected by mineral cations (Na^+, K^+, Mg^{2+}, Ca^{2+}), only included in E4C. These shift NH_4^+_as to the gas phase in high sea salt regions.
- **NH_4^+_as**: Inverse patterns to NH_3; long-range transport suppressed in E4C. Surface deviations >100%, and up to 35% zonal mean, and <5% in UTLS—consistent with ammonium nitrate partitioning behavior.
- **SO_2**: Minor differences, mostly negligible, except for East China, where notable differences are found (> 10%) with zonal mean changes (< 2%) over the Northern Hemisphere. Differences are most likely caused by cloud acidity feedback (via wet chemistry) impacting SO_2 oxidation. Full pH coupling remains to be activated.
- **SO_4^{2-}_as** : Negligible surface/zonal differences (< 1%) consistent with sulfate's non-volatility and weak partitioning dependence.
- **O_3**: Surface and zonal deviations < 0.1%.
- **Regional comparison:** The E4C results are closest to EMEP observations for HNO_3 and NH_4^+_as.

As these are preliminary results, the concentrations shown may evolve with further model refinement.

Further work will focus on:

- Reviewing tracer coupling and implicit parameterizations (e.g., transfer timescales),
- Fine-tuning chemical speciation (sensitive to model resolution and deposition processes),
- Completing code cleaning and integration steps.

5 References

Flemming, J., Huijnen, V., Arteta, J., Bechtold, P., Beljaars, A., Blechschmidt, A.-M., Diamantakis, M., Engelen, R. J., Gaudel, A., Inness, A., Jones, L., Josse, B., Katragkou, E., Marecal, V., Peuch, V.-H., Richter, A., Schultz, M. G., Stein, O., and Tsikerdekis, A.: Tropospheric chemistry in the Integrated Forecasting System of ECMWF, Geosci. Model Dev., 8, 975–1003, https://doi.org/10.5194/gmd-8-975-2015, 2015.

Friese, E. and Ebel, A.: Temperature Dependent Thermodynamic Model of the System H+-NH-Na+-SO-NO-Cl−-H2O, J. Phys. Chem. A, 114, 11595–11631, https://doi.org/10.1021/jp101041j, 2010.

Huijnen, V., Flemming, J., Chabrillat, S., Errera, Q., Christophe, Y., Blechschmidt, A.-M., Richter, A., and Eskes, H.: C-IFS-CB05-BASCOE: stratospheric chemistry in the Integrated Forecasting System of ECMWF, Geosci. Model Dev., 9, 3071–3091, https://doi.org/10.5194/gmd-9-3071-2016, 2016.

Huijnen, V., Le Sager, P., Köhler, M. O., Carver, G., Rémy, S., Flemming, J., Chabrillat, S., Errera, Q., and van Noije, T.: OpenIFS/AC: atmospheric chemistry and aerosol in OpenIFS 43r3, Geosci. Model Dev., 15, 6221–6241, https://doi.org/10.5194/gmd-15-6221-2022, 2022.

Metzger, S., Mihalopoulos, N., and Lelieveld, J.: Importance of mineral cations and organics in gas-aerosol partitioning of reactive nitrogen compounds: case study based on MINOS results, Atmos. Chem. Phys., 6, 2549–2567, https://doi.org/10.5194/acp-6-2549-2006, 2006.

Metzger and Lelieveld, 2007 Metzger, S. and Lelieveld, J.: Reformulating atmospheric aerosol thermodynamics and hygroscopic growth into fog, haze and clouds, Atmos. Chem. Phys., 7, 3163–3193, https://doi.org/10.5194/acp-7-3163-2007, 2007.

Metzger, S., Steil, B., Xu, L., Penner, J. E., and Lelieveld, J.: New representation of water activity based on a single solute specific constant to parameterize the hygroscopic growth of aerosols in atmospheric models, Atmos. Chem. Phys., 12, 5429–5446, https://doi.org/10.5194/acp-12-5429-2012, 2012.

Metzger, S., Steil, B., Abdelkader, M., Klingmüller, K., Xu, L., Penner, J. E., Fountoukis, C., Nenes, A., and Lelieveld, J.: Aerosol water parameterisation: a single parameter framework, Atmos. Chem. Phys., 16, 7213–7237, https://doi.org/10.5194/acp-16-7213-2016, 2016a.

Metzger, S., Abdelkader, M., Klingmueller, K., Steil, B., and Lelieveld, J.: Comparison of Metop PMAp Version 2 AOD Products using Model Data, https://www.eumetsat.int/PMAp, final Report ITT 15/210839, EUMETSAT, 2016b.

Metzger, S., Abdelkader, M., Steil, B., and Klingmüller, K.: Aerosol water parameterization: long-term evaluation and importance for climate studies, Atmos. Chem. Phys., 18, 16747–16774, https://doi.org/10.5194/acp-18-16747-2018, 2018.

Metzger, S., Remy, S., Williams, J. E., Huijnen, V., Meziane, M., Kipling, Z., Flemming, J., and Engelen, R.: Representing acidity in the IFS using a coupled IFS-EQSAM4Clim approach, other, display, https://doi.org/10.5194/egusphere-egu22-11122, 2022.

Metzger, S., Rémy, S., Huijnen, V., Williams, J., Chabrillat, S., Bingen, C., and Flemming, J.: Impact of pH computation from EQSAM4Clim on inorganic aerosols in the CAMS system, other, pico, https://doi.org/10.5194/egusphere-egu23-16085, 2023a.

Metzger, S.: The EQSAM Box Model (for EQSAM4Clim-v12), Zenodo, https://doi.org/10.5281/zenodo.10276178, 2023b.

Metzger, S., Rémy, S., Williams, J. E., Huijnen, V., and Flemming, J.: A computationally efficient parameterization of aerosol, cloud and precipitation pH for application at global and regional scale (EQSAM4Clim-v12), Geosci. Model Dev., 17, 5009–5021, https://doi.org/10.5194/gmd-17-5009-2024, 2024.

Pringle, K. J., Tost, H., Message, S., Steil, B., Giannadaki, D., Nenes, A., Fountoukis, C., Stier, P., Vignati, E., and Lelieveld, J.: Description and evaluation of GMXe: a new aerosol submodel for global simulations (v1), Geosci. Model Dev., 3, 391–412, https://doi.org/10.5194/gmd-3-391-2010, 2010a.

Pringle, K. J., Tost, H., Metzger, S., Steil, B., Giannadaki, D., Nenes, A., Fountoukis, C., Stier, P., Vignati, E., and Lelieveld, J.: Corrigendum to ”Description and evaluation of GMXe: a new aerosol submodel for global simulations (v1)” published in Geosci. Model Dev., 3, 391–412, 2010, Geosci. Model Dev., 3, 413–413, https://doi.org/10.5194/gmd-3-413-2010, 2010b.

Pye, H. O. T., Nenes, A., Alexander, B., Ault, A. P., Barth, M. C., Clegg, S. L., Collett Jr., J. L., Fahey, K. M., Hennigan, C. J., Herrmann, H., Kanakidou, M., Kelly, J. T., Ku, I.-T., McNeill, V. F., Riemer, N., Schaefer, T., Shi, G., Tilgner, A., Walker, J. T., Wang, T., Weber, R., Xing, J., Zaveri, R. A., and Zuend, A.: The acidity of atmospheric particles and clouds, Atmospheric Chemistry and Physics, 20, 4809–4888, https://doi.org/10.5194/acp-20-4809-2020, 2020.

Rémy, S., Kipling, Z., Flemming, J., Boucher, O., Nabat, P., Michou, M., Bozzo, A., Ades, M., Huijnen, V., Benedetti, A., Engelen, R., Peuch, V.-H., and Morcrette, J.-J.: Description and evaluation of the tropospheric aerosol scheme in the European Centre for Medium-Range Weather Forecasts (ECMWF) Integrated Forecasting System (IFS-AER, cycle 45R1), Geosci. Model Dev., 12, 4627–4659, https://doi.org/10.5194/gmd-12-4627-2019, 2019.

Rémy, S., Kipling, Z., Huijnen, V., Flemming, J., Nabat, P., Michou, M., Ades, M., Engelen, R., and Peuch, V.-H.: Description and evaluation of the tropospheric aerosol scheme in the Integrated Forecasting System (IFS-AER, cycle 47R1) of ECMWF, Geosci. Model Dev., 15, 4881–4912, https://doi.org/10.5194/gmd-15-4881-2022, 2022.

Rémy, S., Metzger, S., Huijnen, V., Williams, J. E., and Flemming, J.: An improved representation of aerosol in the ECMWF IFS-COMPO 49R1 through the integration of EQSAM4Climv12 – a first attempt at simulating aerosol acidity, Geosci. Model Dev., 17, 7539–7567, https://doi.org/10.5194/gmd-17-7539-2024, 2024.

Wexler, A. S. and Clegg, S. L.: Atmospheric aerosol models for systems including the ions H+, NH4+, Na+, SO42−, NO3−, Cl−, Br−, and H2O, J. Geophys. Res.-Atmos., 107, ACH 14-1–ACH 14-14, https://doi.org/10.1029/2001JD000451, 2002.

Williams, J. E., Huijnen, V., Bouarar, I., Meziane, M., Schreurs, T., Pelletier, S., Marécal, V., Josse, B., and Flemming, J.: Regional evaluation of the performance of the global CAMS chemical modeling system over the United States (IFS cycle 47r1), Geoscientific Model Development, 15, 4657–4687, https://doi.org/10.5194/gmd-15-4657-2022, 2022.

Williams, J., Metzger, S., Rémy, S., Huijnen, V., and Flemming, J.: An evaluation of the regional distribution and wet deposition of secondary inorganic aerosols and their gaseous precursors in IFS-COMPO Cycle 49R1, Geosci. Model Dev. Discuss. [preprint], https://doi.org/10.5194/gmd-2024-188, in review, 2024.

Document History

Version	Author(s)	Date	Changes
1.0	Swen Metzger, Vincent Huijnen, Ramiro Checa-Garcia, Samuel Rémy	17-06-2025	Initial version
1.1	Swen Metzger	27-06-2025	New version after internal review

Internal Review History

Internal Reviewers	Date	Comments
R. Jansen	26-06-2025	Small comments